



N-acyl-homoserine lactones in extracellular polymeric substances from sludge for enhanced chloramphenicol-degrading anode biofilm formation in microbial fuel cells

Xiayuan Wu^a, Lina Zhang^a, Zuopeng Lv^b, Fengxue Xin^a, Weiliang Dong^a, Guannan Liu^{a,c}, Yan Li^a, Honghua Jia^{a,*}

^a College of Biotechnology and Pharmaceutical Engineering, Nanjing Tech University, Nanjing, 211816, China

^b The Key Laboratory of Biotechnology for Medicinal Plants of Jiangsu Province, Jiangsu Normal University, Xuzhou, 221116, China

^c Frontier Technology Research Institute, Tianjin University, Tianjin, 301700, China

ARTICLE INFO

Keywords:

AHLs
Quorum sensing
Extracellular polymeric substances
Microbial fuel cell
Chloramphenicol degradation
Electrode biofilm

ABSTRACT

Exploring an efficient acclimation strategy to obtain robust bioanodes is of practical significance for antibiotic wastewater treatment by bioelectrochemical systems (BESs). This study investigated the effects of two acclimation conditions on chloramphenicol (CAP)-degrading anode biofilm formation in microbial fuel cells (MFCs). The one was continuously added the extracellular polymeric substances (EPS) extracted from anaerobic sludge and increasing concentrations of CAP after the first start-up phase, while the other was added the EPS-1 (N-acyl-homoserine lactones, namely AHLs were extracted from the EPS) at the same conditions. The results demonstrated that AHLs in the sludge EPS played a crucial role for enhanced CAP-degrading anode biofilm formation in MFCs. The AHL-regulation could not only maintain stable voltage outputs but also significantly accelerate CAP removal in the EPS MFC. The maximum voltage of 653.83 mV and CAP removal rate of 1.21 ± 0.05 mg/L-h were attained from the EPS MFC at 30 mg/L of CAP, which were 0.84 and 1.57 times higher than those from the EPS-1 MFC, respectively. These improvements were largely caused by the thick and 3D structured biofilm, strong and homogeneous cell viability throughout the biofilm, and high protein/polysaccharide ratio along with more conductive contents in the biofilm EPS. Additionally, AHLs facilitated the formation of a biofilm with rich biodiversity and balanced bacterial proportions, leading to more beneficial mutualism among different functional bacteria. More bi-functional bacteria (for electricity generation and antibiotic resistance/degradation) were specifically enriched by AHLs as well. These findings provide quorum sensing theoretical knowledge and practical instruction for rapid antibiotic-degrading electrode biofilm acclimation in BESs.

1. Introduction

The global consumption of antibiotics is continuously increasing, posing a huge threat to the environment by releasing antibiotic wastewaters (Ondon et al., 2020; Zhu et al., 2017). Chloramphenicol (CAP), a typical chlorinated nitroaromatic antibiotic, has been widely applied for human and animal infectious diseases around the world due to its broad-spectrum antibacterial property and low price (Liu et al., 2018a). Consequently, the frequent detection of CAP (ranging from ng/L to mg/L) in different aquatic environments, such as surface and underground waters, domestic wastewater effluents, and pharmaceutical wastewaters, has been reported (Kong et al., 2015). In order to remove

CAP from these water matrices, considerable methods have been explored, including Fenton degradation, photocatalytic degradation, electrochemical degradation, microbial degradation, and so on (Her-raiz-Carbone et al., 2020; Hu et al., 2020; Kumar et al., 2020; Zhang et al., 2020a). These sophisticated methods, however, are limited in practical application because of high energy consumptions, large chemical needs, and potential secondary pollution.

Recently, bioelectrochemical systems (BESs), as an environment-friendly technology, show great potential for antibiotic removal and antibiotic resistance genes (ARGs) reduction due to the combination functions of microbial metabolism and electrochemical redox reactions (Yan et al., 2019). Till now, two main kinds of BESs, including microbial

* Corresponding author. Nanjing Tech University, No.30 Puzhu Road (S), Nanjing, 211816, Jiangsu, PR China.

E-mail addresses: wuxiayuan@njtech.edu.cn (X. Wu), hjia@njtech.edu.cn (H. Jia).

<https://doi.org/10.1016/j.envres.2021.112649>

Received 28 September 2021; Received in revised form 21 December 2021; Accepted 28 December 2021

Available online 31 December 2021

0013-9351/© 2021 Elsevier Inc. All rights reserved.

fuel cells (MFCs) and microbial electrolysis cells (MECs), have been utilized for antibiotic wastewater treatment (Yan et al., 2019). CAP can be degraded by both the bioanode of MFCs and the biocathode of MECs (Liang et al., 2013; Zhang et al., 2017). A large proportion of studies have focused on optimizing operational conditions of BESs to enhance CAP removal efficiency (Guo et al., 2017; Liang et al., 2013; Zhang et al., 2017). Nevertheless, electrode biofilms (anode and cathode biofilms), as a vital role for electrochemical reactions and CAP degradation in BESs, have gained less attention (Chatterjee et al., 2019). Yun et al. (2016) proposed to efficiently get a biocathode for CAP removal in MECs by inverting a CAP-degrading bioanode from MFCs. Accordingly, an efficient acclimation strategy for CAP-degrading bioanode in MFCs is of practical significance to acquire electrode biofilms. Generally, the antibiotic-degrading bioanodes in MFCs still exist some shortcomings, such as prolonged acclimation time, low antibiotic tolerance, and poor shock resistance (Yan et al., 2019). Lately, we established a novel synchronous acclimation strategy for CAP-degrading bioanodes through the continuous addition of sludge and increasing concentrations of CAP in MFCs; thereafter, the acclimation time was shortened by 1.52 times, meanwhile the obtained CAP-degrading bioanode showed high CAP tolerance (80 mg/L) and robust shock resistance (keeping stable voltage outputs during the whole acclimation time); the continuous addition of sludge was the key reason to cause better biofilm properties and bacterial mutualism (Wu et al., 2021). Hence, this previous work triggered us to think: what in sludge did play a critical role in enhanced CAP-degrading anode biofilm formation in MFCs?

Extracellular polymeric substances (EPS), mainly composed of polysaccharide (PS) and protein (PN), are an important component for various kinds of sludge. EPS have been recognized to act a key role in the formation of granular sludge and biofilms for wastewater treatment (Jia et al., 2017). It is recently found that the exogenous EPS from sludge can improve anammox microbial activity and maintain sludge structural stability (J. Guo et al., 2016a, 2016b; Liu et al., 2018b; Zhang et al., 2020b). On the other hand, N-acyl-homoserine lactones (AHLs), a kind of quorum sensing (QS) signal molecules for cell-to-cell communication of gram-negative bacteria, widely exist in EPS from sludge (Liu et al., 2018b). An increasing number of studies have demonstrated that AHL-mediated QS can regulate various microbial behaviors including EPS secretion, biofilm formation, recalcitrant pollutant degradation, and microbial community construction (Xiong et al., 2020). In particular, as the majority of known electroactive microorganisms are gram-negative, the addition of exogenous AHLs can improve the performance of BESs by increasing the production of electron shuttles (for pure culture), promoting the abundance of electroactive bacteria (for mixed culture), and bettering the biofilm properties (e.g., high cell viability, more biomass and EPS) (Chen et al., 2017; Fang et al., 2018; Venkataraman et al., 2010). But to the best of our knowledge, very little attention has been paid to the antibiotic-degrading electrode biofilm formation influenced by AHLs in BESs. Since AHLs and EPS have some consistent influences relating to the biofilm formation and adverse environment resistance, it is logical to presume that AHLs existing in EPS from sludge might be the key manipulator for enhanced CAP-degrading anode biofilm formation in our previous study (Wu et al., 2021).

Therefore, this study aims to validate the above hypothesis. Based on the synchronous acclimation strategy in our previous study, the EPS extracted from anaerobic sludge were continuously added with increasing concentrations of CAP after the first start-up phase to acclimate the CAP-degrading bioanode in MFCs. For comparison, the EPS-1 (AHLs were extracted from the EPS) were added with CAP at the same conditions in another group. The performance of the MFCs was evaluated according to electrochemical characteristics and CAP removal ability. The biofilm properties were comprehensively estimated through the analyses of morphology, viability, and EPS production. In combination with the microbial community analysis, the function mechanisms of AHLs in the sludge EPS for CAP-degrading anode biofilm formation were unfolded.

2. Materials and methods

2.1. EPS extraction from sludge

The anaerobic digester sludge used in the experiments was taken from the Nanjing Jiangxinzhou wastewater treatment plant (Jiangsu, China). EPS were extracted from the sludge using an EDTA method (Yang et al., 2019). Briefly, 50 mL sludge was mixed with 5 mL 2% EDTA solution for shaking 5 h, followed by centrifugation at 8000 rpm for 20 min. The obtained supernatant (about 50 mL) was then filtered through 0.22 μm membrane filters and collected as the EPS.

2.2. Extraction and identification of AHLs in sludge EPS

AHLs from the EPS were extracted with an equal volume of ethyl acetate. The solvent extracts were evaporated using a rotary evaporator at 40 $^{\circ}\text{C}$, and redissolved in 1 mL methanol for analysis. The rest EPS solution was collected as the EPS without AHLs, which was noted the "EPS-1".

In order to determinate whether AHLs were extracted from the EPS, the EPS and EPS-1 were both detected by using AHLs reporter plate bioassay. The AHL-sensing bacterium *Agrobacterium tumefaciens* KYC55, provided by Prof. Jun Zhu (Nanjing Agricultural University, Nanjing, China), was cultured in LB agar medium overnight at 30 $^{\circ}\text{C}$, then X-gal, and EPS or EPS-1 were added to the agar plate (Chen et al., 2017). The AHLs extracts from the EPS were identified by using an ultra-performance liquid chromatography-tandem mass spectrometric (UPLC-MS/MS) system (Xevo TQ-XS, Waters, USA) as described by Wang et al. (2021).

2.3. MFC construction and operation

This study used two-chamber MFCs (each chamber: 70 mL) which were described in our previous work (Wu et al., 2018). A proton exchange membrane (Nafion 117, Dupont Co., USA) was applied to separate the anode and cathode chambers. The anode and cathode electrodes were graphite felts (4.0 cm \times 4.0 cm \times 0.5 cm; Hunan Jihua Carbon Hi-Tech Co., Ltd., China). The normal anolyte was 50 mM phosphate buffer (PBS, pH = 7.0) containing 1 g/L of glucose, while the catholyte consisted of 50 mM PBS and 50 mM ferricyanide (Wu et al., 2018). The external resistance and operational temperature for all MFCs were 1000 Ω and 30 \pm 0.5 $^{\circ}\text{C}$, respectively.

2.4. Acclimation experiment

Based on the synchronous acclimation strategy in our previous study, the acclimation process for all the experimental groups included two phases. In the first phase, all the experimental groups followed the same procedure: the anode chamber was filled with a mixture of the anaerobic digester sludge and the normal anolyte supplemented with 1 mg/L of CAP (volume ratio = 1:2); the first start-up phase of the MFCs was considered to be finished as stable voltage outputs were attained (Wu et al., 2021). In the second phase, the EPS or EPS-1, instead of the anaerobic digester sludge, and the normal anolyte supplemented with gradually increasing concentrations of CAP (5, 10, 15, 20, 25, 30 mg/L) were continuously added to the anode chamber, which was labelled as the EPS or EPS-1 MFC group, respectively. For comparison, a control group only added the normal anolyte amended with gradually increasing concentrations of CAP (5, 10, 15 mg/L) in the second phase was carried out at the mean time. The different concentrations of CAP applied in the test (EPS and EPS-1) and control groups during the second phase were attributed to the corresponding MFC performance, as the added concentration of CAP was not increased until the voltage outputs of the MFC kept steady. All MFC reactors were conducted in a batch-fed mode (3 days for each cycle).

2.5. Analytical methods

The voltage outputs, polarization and power density curves of MFCs were obtained according to the methods described in our previous study (Wu et al., 2021). Cyclic voltammetry (CV) and electrochemical impedance spectroscopy (EIS) were carried out in a three-electrode system as described in our previous study (Cui et al., 2020). The CV was conducted following the conditions: scan rate of 10 mV/s and potential range of $-800 \sim +800$ mV. The EIS conditions were as follows: potential amplitude of 10 mV and frequency range of 100 kHz–5 mHz.

The CAP concentration was analyzed by high-performance liquid chromatography (HPLC; Agilent 1260LC, Santa Clara, CA, USA) (Wu et al., 2021). A scanning electron microscopy (SEM, Hitachi S-4800, Japan) was used to observe the morphology of different anode biofilms. A confocal laser scanning microscopy (CLSM, Ultra View VOX, PE, USA) was utilized to view the distributions of (dead and live) cells and EPS components (PS, PN, and lipids) in different anode biofilms according to the procedures in previous work (Wu et al., 2021).

The phenol-sulfuric acid method and a BCA Protein Assay Kit (Beyotime Biotechnology, China) were used to determine the PS and PN

contained in the EPS of the biofilms, respectively (Wu et al., 2021). A Cary Eclipse fluorescence spectrophotometer (Varian, USA) was applied to further analyze the three-dimensional excitation emission matrix (3D-EEM) of the biofilm EPS following detailed conditions mentioned in our previous study (Wu et al., 2021). The intracellular protein concentration of the biofilms was also analyzed by the BCA Protein Assay Kit to evaluate the biomass of the biofilms (Wu et al., 2015).

2.6. Microbial community analysis

The different anode biofilms (three biological repetitions for each sample) were sampled at the end of the experiments to extract the total DNA for microbial community analysis. A set of archaeal and bacterial primers 515 F and 806 R was used to amplify the hypervariable V4 region of 16 S rRNA gene. The detailed procedures for the 16 S rRNA gene high throughput sequencing experiments and raw data analysis were depicted in our previous work (Wu et al., 2020).

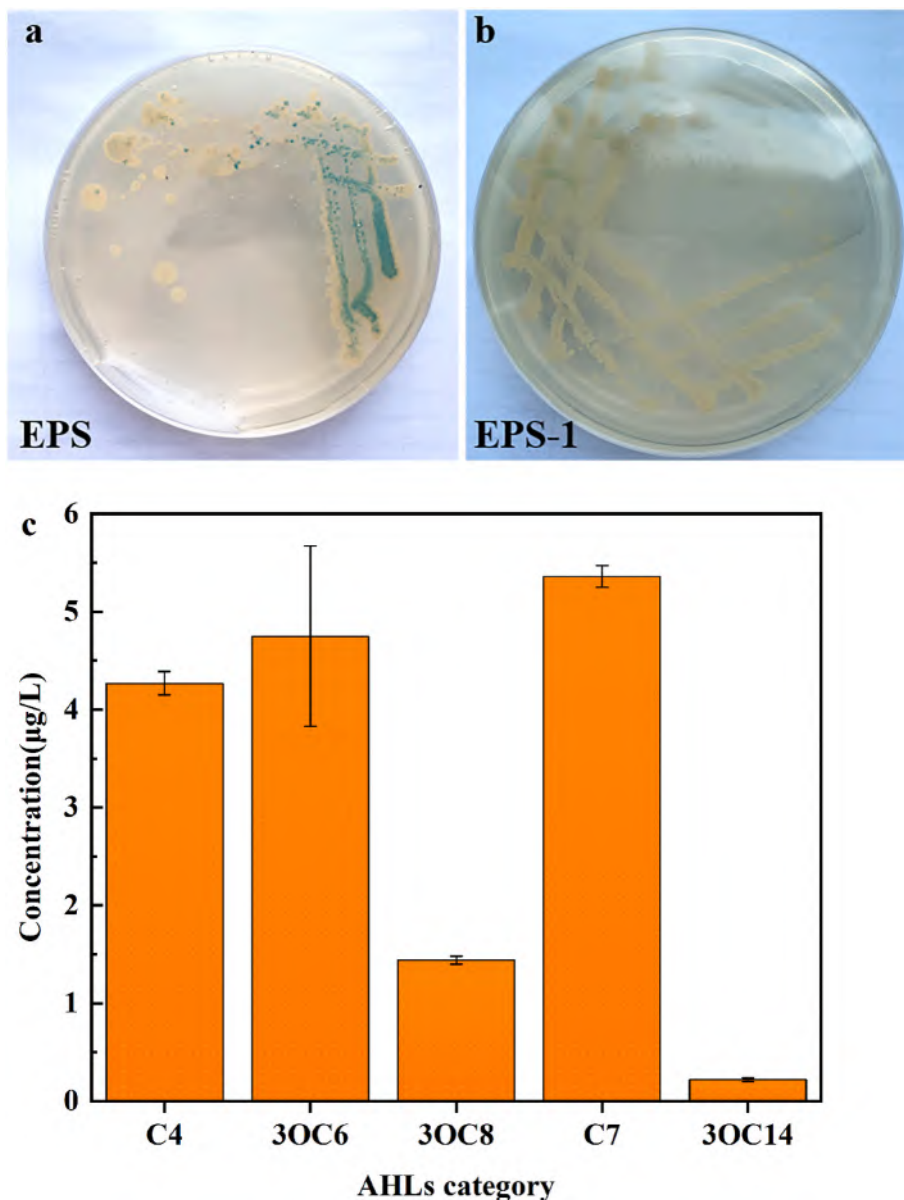


Fig. 1. AHLs detection by the agar plate-based bioassay (a, b) and UPLC-MS/MS analysis (c).

3. Results and discussion

3.1. Identification of AHLs in EPS from sludge

In order to provide the direct evidence about the existence of AHLs, the EPS and EPS-1 were detected according to the agar-plate based bioassay using biosensor *A. tumefaciens* KYC55. As a result (Fig. 1a and b), the agar-plate for the EPS clearly showed blue color, while the agar-plate for the EPS-1 had no color reaction. This indicated that AHLs were not detected in the EPS-1. Therefore, AHLs were efficiently extracted from the EPS by ethyl acetate. UPLC-MS/MS was applied to further clarify the AHLs species in the EPS. As shown in Fig. 1c, five kinds of AHLs were identified in the EPS, displayed in a decreasing order of concentration as C7-HSL ($5.36 \pm 0.11 \mu\text{g/L}$), 3OC6-HSL ($4.75 \pm 0.92 \mu\text{g/L}$), C4-HSL ($4.27 \pm 0.12 \mu\text{g/L}$), 3OC8-HSL ($1.44 \pm 0.04 \mu\text{g/L}$), and 3OC14-HSL ($0.22 \pm 0.02 \mu\text{g/L}$). Wang et al. (2021) also found that C7-HSL, 3OC6-HSL, C4-HSL, and 3OC8-HSL were the main kinds of AHLs in sludge; furthermore, the short-chain AHLs (C4–C10) normally had higher concentrations than the long-chain AHLs (C12–C14), which was consistent with the results in this study.

3.2. Effects of AHLs on electricity generation

From Fig. 2a, the EPS MFC generated relatively steady voltages in the whole operation cycles, while the other two MFC groups had fluctuant voltage outputs, especially in the later period with higher CAP concentrations. This implied that the acclimated bioanode in the EPS MFC was

robust to the increasing concentrations of CAP. For the EPS MFC, the maximum voltage (705.64 mV) was obtained at 25 mg/L of CAP, and the maximum voltage slightly decreased to 653.83 mV at the end of acclimation time (30 mg/L of CAP). The maximum voltages from the EPS-1 and control MFCs at the end of acclimation time only reached 354.88 and 345.12 mV, respectively. The polarization and power density plots in the last operation cycle (Fig. 2b) indicated that the highest power density (182.25 mW/m^2) was obtained from the EPS MFC, which was 1.68 times as high as that from the control MFC (108.73 mW/m^2).

Based on the CV curves (Fig. 2c), the EPS bioanode had the largest double layer capacitance and peak current, implying it possessed the strongest electrochemical activity. A pair of clear redox peaks observed from the EPS bioanode centered at about 0.10 and 0.25 V (vs. Ag/AgCl) with currents of -0.0048 and 0.0051 A, respectively. According to the EIS curves (Fig. 2d), the ohmic resistance (R_s), charge-transfer resistance (R_{ct}), and diffusion resistance (W) of the EPS bioanode were 2.09, 5.92, and 2.01Ω , respectively. On the contrary, those of the control bioanode increased to 6.92, 15.59, and 19.02Ω , respectively. Accordingly, the stable and high electrochemical performance from the EPS MFC under increasing concentrations of CAP revealed the EPS biofilm had stronger CAP tolerance than the EPS-1 and control biofilms. Besides, AHLs rather than other contents in the EPS from sludge played a critical role in the robust anode biofilm construction in CAP-degrading MFCs. Pan et al. (2020) also confirmed that the addition of AHLs enhanced the electricity generation (up to 62%) of the electroactive biofilms after high toxicity shock in MFC biosensors, which was similar with the increase (67.62%) of the EPS MFC in this study. However, Chen et al. (2017) reported a

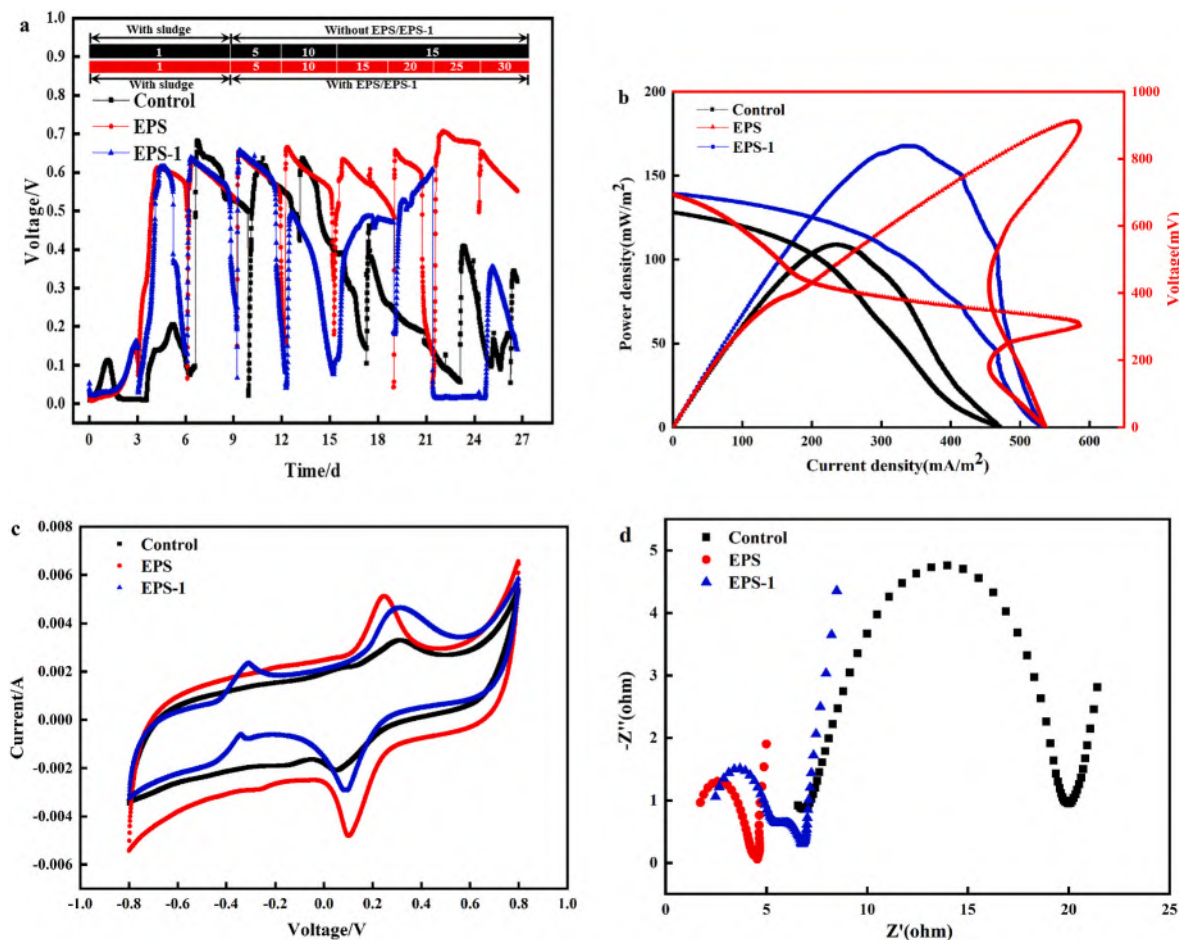


Fig. 2. Voltage output (a), polarization and power density (b), cyclic voltammogram (c), and electrochemical impedance spectroscopy (d) curves of the MFCs with different acclimation conditions; the black (for Control) and red (for EPS and EPS-1) stripes in voltage output curves (a) indicate the CAP concentrations (mg/L) at corresponding acclimation time. (For interpretation of the references to color in this figure legend, the reader is referred to the Web version of this article.)

relatively low enhancement of electricity generation (up to 27.92%) in MFCs with AHLs addition under non-toxic stress. Thus, the positive effects of exogenous AHLs for electricity generation in MFCs would be more notable under adverse situations.

3.3. Effects of AHLs on CAP removal

The concentration changes of CAP in the different MFCs during the last operation cycle were monitored (Fig. 3a). Clearly, the EPS MFC displayed the fastest CAP removal rate (1.21 ± 0.05 mg/L·h), which was 1.57 and 2.18 times higher than those in the EPS-1 (0.47 ± 0.04 mg/L·h) and control (0.38 ± 0.03 mg/L·h) MFCs, respectively. W. Guo et al. (2016a, 2016b) obtained a removal rate of 0.53 mg/L·h by the MFC bioanode at 30 mg/L of CAP, which was lower than the half of the removal rate from the EPS MFC in this study. The CAP removal data in all MFC groups also fitted the apparent first-order kinetic model very well (Fig. 3b). Table S2 (Supporting Information) presents the linear fitting results of all MFCs. The removal rate constant of the EPS MFC (0.14 h⁻¹) nearly doubled that of the control MFC (0.09 h⁻¹). Besides, the removal rate constant of the EPS MFC was similar with that of the MFC with continuous sludge addition (0.11 h⁻¹) in our previous study (Wu et al., 2021). These results implied that the continuous addition of the sludge EPS, specifically AHLs in the sludge EPS, remarkably promoted CAP removal ability of the MFC bioanode during the acclimation process. Previous studies have been verified that exogenous AHLs can strengthen the microbial degradation of refractory organic pollutants

(Lv et al., 2021; Maddela et al., 2019).

3.4. Effects of AHLs on CAP-degrading anode biofilms

As displayed in Fig. 4a, unlike the other two groups, the EPS group possessed a significantly thick and 3D structured biofilm; although some cocci were also found, a larger quantity of rod-shaped bacterial cells formed multi-layer loose and porous structure, which was similar with the biofilm acclimated through continuously adding sludge in our previous work (Wu et al., 2021). This distinctive biofilm structure can result in high permeability and cell viability (Wu et al., 2021). Conversely, the bacterial cells in the EPS-1 and control biofilms aggregated together to form tight and dense structure, which was ascribed to the substantial amount of sticky bacterial secretions that enwrapped cells. These sticky bacterial secretions have been demonstrated to be PS for cell-protection under environmental stress (Wu et al., 2021). The SEM results indicated that AHLs in the EPS improved bacterial attachment on the electrode, and facilitated the construction of a 3D structured biofilm. Xiong et al. (2020) also found that the addition of exogenous AHLs accelerated the formation of thick and structured biofilms on carriers.

As can be seen from Fig. 4b, the EPS biofilm had a greater quantity of metabolically energetic cells compared to the other two biofilms. Furthermore, the EPS biofilm showed a homogeneous active state, while the other two biofilms inclined to shape a typical “two-layer” biofilm (the inner dead cells and the outer live cells) (Sun et al., 2015). This similar phenomenon was also observed in our previous work (Wu et al., 2021). The thicknesses of the EPS, EPS-1, and control biofilms were 27.6, 21.5, and 20.1 μm , respectively. Besides, the intracellular protein concentrations of the EPS, EPS-1, and control biofilms were 100.51, 86.92, and 76.33 $\mu\text{g/L}\cdot\text{cm}^2$, respectively. This further confirmed that the EPS biofilm had the largest amount of biomass. Therefore, AHLs in the EPS increased the biomass and proportion of live cells for the biofilm. Similar results were also obtained in *Geobacter soli* cathode biofilms acclimated by AHLs addition (Fang et al., 2018).

It is well known that the microbial enrichment and biofilm formation are critically influenced by EPS (Zhang et al., 2019b). CLSM was also applied to analyze the EPS components distribution in different anode biofilms (Fig. 4c). The EPS biofilm was occupied by a majority of PN, and a small part of PS and lipids. Contrarily, more PS and lipids were found in both the EPS-1 and control biofilms.

The EPS concentrations in the different anode biofilms were further quantified (Fig. 5a). The total EPS concentration was noticeably higher in the EPS biofilm compared with that in the EPS-1 and control biofilms, which was mainly due to the differences of PN. This was in good agreement with the results of CLSM for EPS. The PN of the EPS biofilm achieved 192.10 ± 2.31 $\text{mg L}^{-1}\cdot\text{cm}^{-2}$, while the PN in the EPS-1 and control biofilms were only 71.20 ± 6.54 and 36.08 ± 3.33 $\text{mg L}^{-1}\cdot\text{cm}^{-2}$, respectively. By contrast, the PS in the EPS biofilm (6.11 ± 3.45 $\text{mg L}^{-1}\cdot\text{cm}^{-2}$) was remarkably lower compared to that in the EPS-1 (19.04 ± 3.46 $\text{mg L}^{-1}\cdot\text{cm}^{-2}$) and control (50.89 ± 2.31 $\text{mg L}^{-1}\cdot\text{cm}^{-2}$) biofilms. Our previous study has demonstrated that a higher PN/PS ratio facilitated the CAP-degrading anode biofilm formation, which was also confirmed in this work (Wu et al., 2021). This can be explained by that the electron transfer is mainly mediated through the outer membrane proteins and extracellular redox-active proteins (Kumar et al., 2017). Fang et al. (2018) also confirmed that AHLs increased PN abundance in the EPS of *G. soli* cathodic biofilms, leading to better electron transfer capacity. Interestingly, it is worth noting that AHLs remarkably promoted PN production but inhibited PS secretion in this study, yet many other studies reported that the secretion of both PN and PS, especially PS, was elevated by exogenous AHLs (Hu et al., 2016; Lv et al., 2021; Xiong et al., 2020). This was probably due to the natural AHLs mixture applied in this work, while many other studies normally used single commercial AHL (such as C4-HSL, C6-HSL, 3OC8-HSL, etc.). Thus, the natural AHLs in the sludge EPS could intelligently regulate EPS synthesis to form a superior biofilm according to specific requirements.

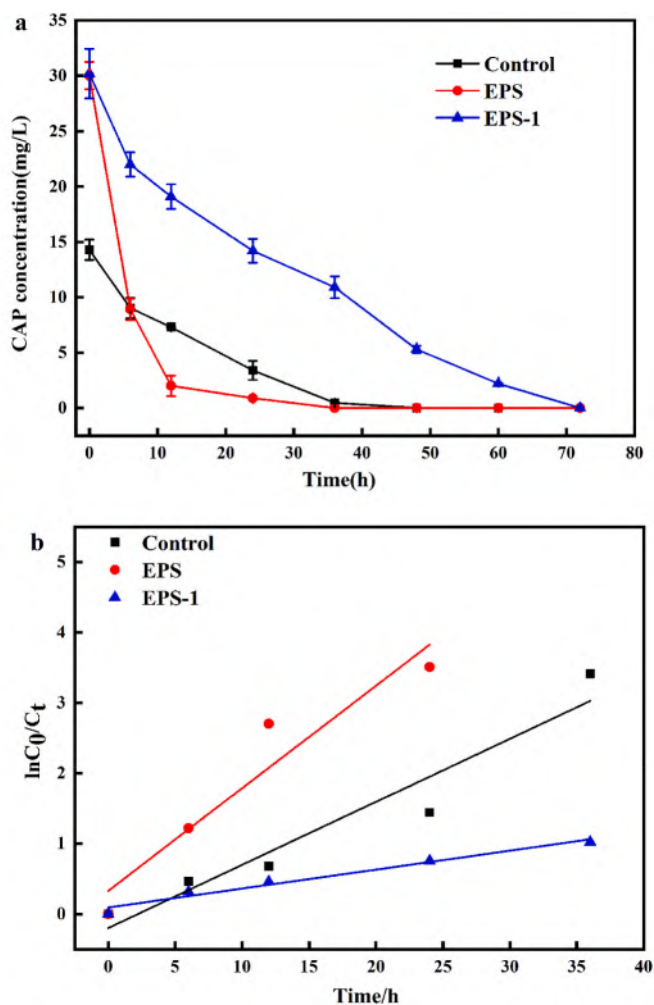


Fig. 3. The concentration changes (a) and kinetics (b) of CAP in the different MFCs during the last operation cycle.

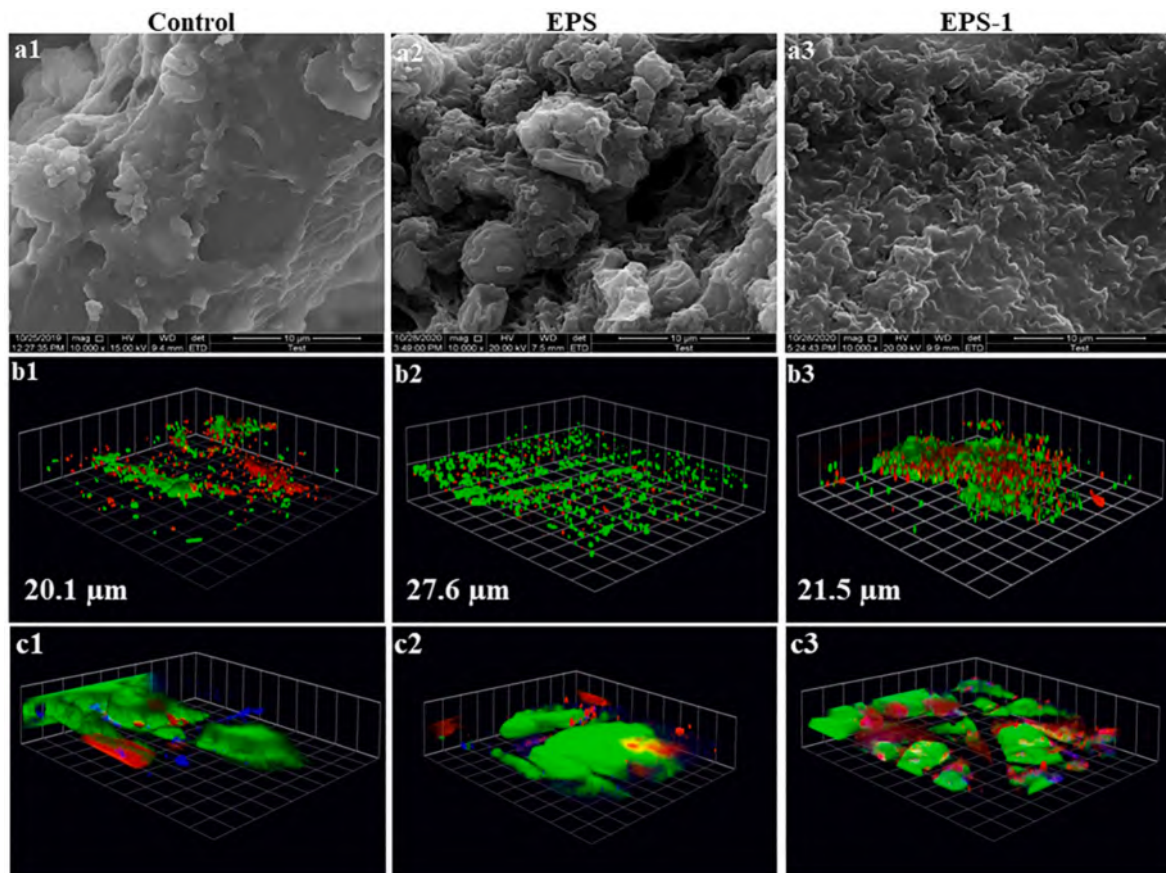


Fig. 4. The images of SEM (a), and CLSM with cells (b; live cells indicated by green, dead cells indicated by red) and EPS (c; polysaccharides indicated by blue, proteins indicated by green, lipids indicated by red) distributions for the different anode biofilms at the end of the operation time. (For interpretation of the references to color in this figure legend, the reader is referred to the Web version of this article.)

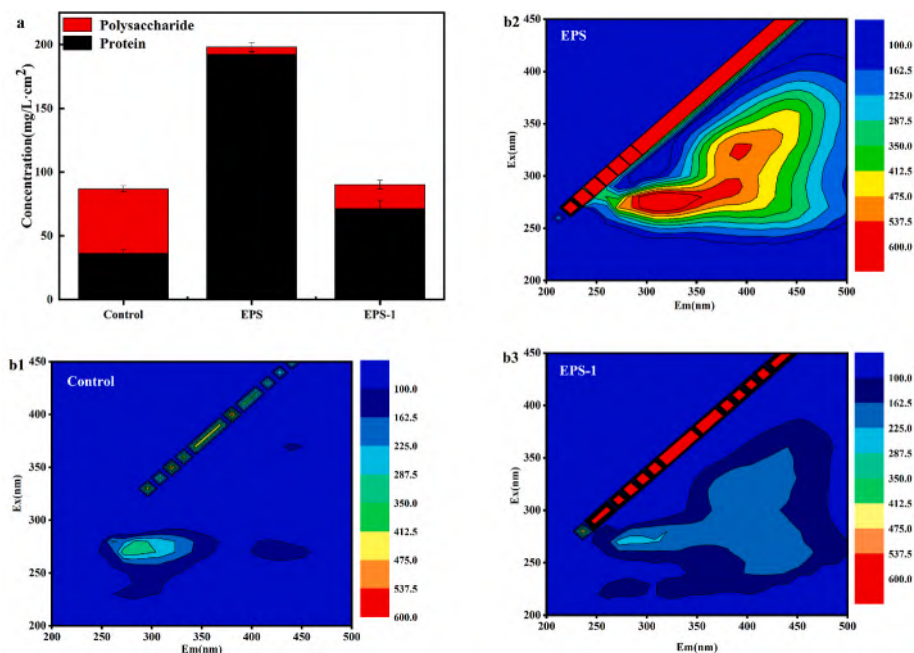


Fig. 5. The component concentrations (a) and 3D-EEM fluorescence spectra (b) of EPS extracted from the different anode biofilms at the end of the operation time.

3D-EEM was also applied to analyze the EPS contents in the different anode biofilms (Fig. 5b). Visibly, more EPS contents were found in the EPS biofilm

(Fig. 5b2), there were mainly two peaks. The peak at the excitation/emission wavelengths (Ex/Em) of 325–400 nm/425–475 nm represented humic acid-like substances (He et al., 2020). The other peak at

the Ex/Em of 275–300 nm/300–375 nm indicated the presence of microbial by-products (e.g., tyrosine-like, tryptophan-like, and protein-like substances) (Zhang et al., 2018). For the EPS-1 biofilm (Fig. 5b3), two similar peaks were also found but with largely declined intensities. Concerning the control biofilm (Fig. 5b1), only one clear peak considered as microbial by-products was observed. Since the proteins and humic acids can efficiently mediate electron transfer, the EPS biofilm with abundant protein-like and humic acid-like substances exhibited high electrochemical activity (Klöpffel et al., 2014; Kumar et al., 2017). Other researchers also deemed that the exogenous AHLs were responsible for promoted conductive contents in the EPS of electroactive biofilms (Chen et al., 2017; Fang et al., 2018).

3.5. Effects of AHLs on microbial community in anode biofilms

The microbial community structures of the different anode biofilms were analyzed by high throughput sequencing at the end of the operation time (Fig. 6). Evidently, there were increased richness and biodiversity in the EPS biofilm compared with the other two groups (Table S3, Supporting Information). Seven main phyla were found in the EPS biofilm: *Proteobacteria* (40.81%), *Actinobacteriota* (27.23%), *Planctomycetota* (6.91%), *Chloroflexi* (6.00%), *Bacteroidota* (4.86%), *Firmicutes* (4.12%), and *Euryarchaeota* (3.20%). For the EPS-1 biofilm, there were three main phyla: *Proteobacteria* (81.84%), *Bacteroidota* (11.37%), and

Actinobacteriota (5.04%). In terms of the control biofilm, there were four main phyla: *Proteobacteria* (45.70%), *Bacteroidota* (37.10%), *Actinobacteriota* (12.38%), and *Firmicutes* (4.37%). The EPS-1 and control biofilms shared the same top 3 phyla, but they showed significant differences from the EPS biofilm. *Proteobacteria*, the most abundant phylum in all samples, has been widely detected in both bioanodes and biocathodes of BESs using for antibiotic removal (Ma et al., 2019; Zhang and Li et al., 2020). *Actinobacteriota*, another dominant phylum in all samples, has been regarded to be active ARGs hosts for antibiotic degradation (Qin et al., 2020; Zhang et al., 2017). *Bacteroidota* and *Firmicutes* both have been reported to have the potential for electricity generation and antibiotic degradation (Guo et al., 2017; Qin et al., 2020). Likewise, *Planctomycetota* and *Chloroflexi* have also been suggested to be potential bi-functional bacteria for electricity generation and antibiotic degradation (Chen et al., 2016; Ren et al., 2021; Zhu et al., 2020). *Euryarchaeota* recently has been found to be the dominant archaea in BESs for antibiotic degradation (Zhao et al., 2019). An increasing number of studies proposed the assignable synergistic role of methanogens for electricity production and antibiotic removal in BESs (Guo et al., 2019; Zhang et al., 2019a). Since phylum *Euryarchaeota* was only found in the EPS biofilm, it suggested that the EPS biofilm possessed ecologically balanced microbial community structures.

From Fig. 6b, the principal genera accounted more balanced proportions in the EPS biofilm, such as *Pseudonocardia* (12.48%), *Chujaibacter*

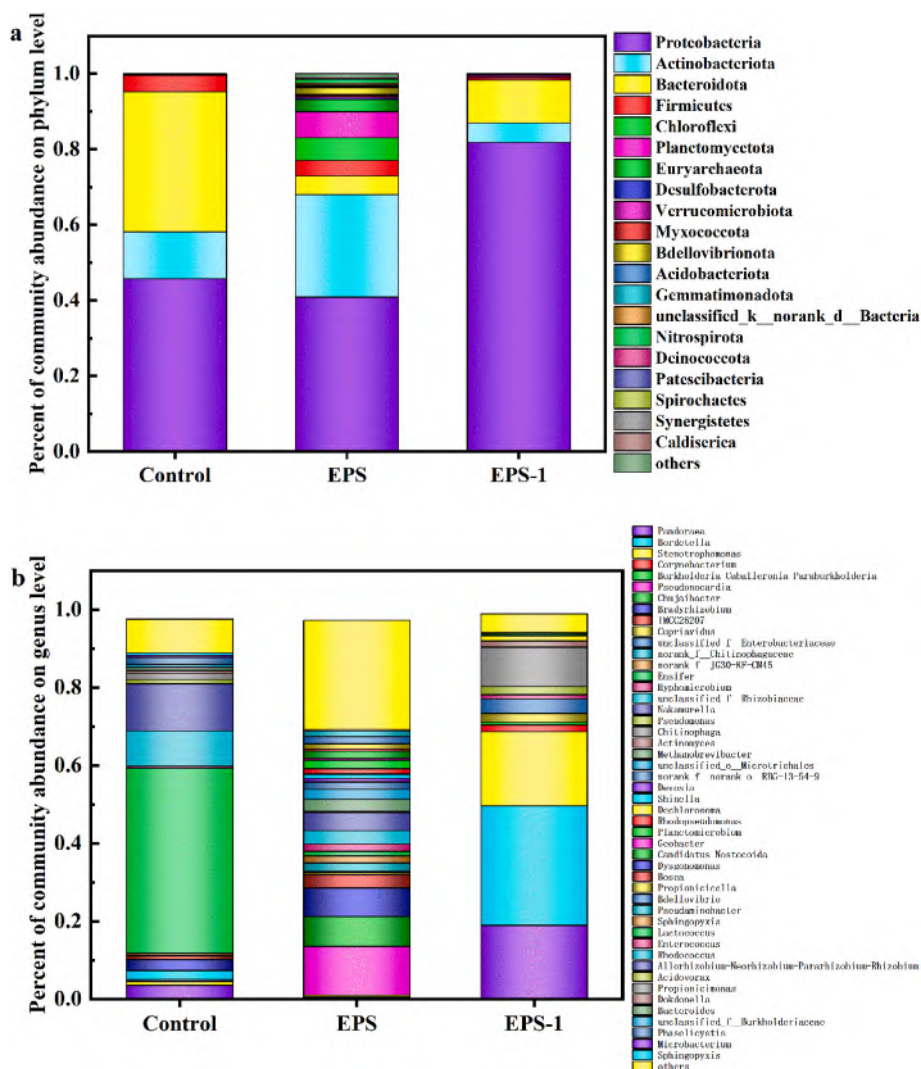


Fig. 6. Microbial community compositions at the phylum (a) and genus (b) levels in the different anode biofilms at the end of the operation time.

(7.64%), *Bradyrhizobium* (7.35%), and the majority of the rest bacteria with similar percentages. As for the EPS-1 biofilm, there were four main genera: *Bordetella* (30.67%), *Stenotrophomonas* (19.02%), *Pandoraea* (18.93%), and *Chitinophaga* (10.12%). For the control biofilm, there were three dominant genera: *Lactococcus* (47.62%), *Allorhizobium-Neorhizobium-Pararhizobium-Rhizobium* (12.07%), and *Rhodococcus* (9.00%). *Pseudonocardia* has been considered to be electroactive bacteria with the ability for lignocellulose degradation and ARGs host (Ma et al., 2020; Zhang et al., 2020c). *Chujaibacter* has been reported to be enriched in a bio-electro-Fenton system for antibiotic degradation (Li et al., 2020). Likewise, *Bradyrhizobium* has been found to be involved in power generation and CAP degradation (Kong et al., 2018; Zhang et al., 2020a). *Bordetella* is known as a kind of pathogen possessing antibiotic resistance, while *Lactococcus* is known as a kind of electroactive bacteria with the ability for quinones production (Dewan et al., 2018; Freguia et al., 2009). *Stenotrophomonas* as a kind of electroactive bacteria has been found to be selected in MFCs for azo dye degradation (Li et al., 2022). *Allorhizobium-Neorhizobium-Pararhizobium-Rhizobium* has been demonstrated to be the dominant potential hosts for some ARGs (Li et al., 2019). These results implied that more bacteria with double functions (electricity generation and antibiotic resistance/degradation) were specifically enriched in the EPS biofilm. Therefore, AHLs in the sludge EPS facilitated the formation of a biofilm with rich biodiversity and balanced bacterial proportions, leading to more beneficial mutualism among different functional bacteria. It has been proven that exogenous AHLs can induce the succession of bacterial community structure to a better direction, facilitating the cooperation and syntrophy among different functional bacteria (Lv et al., 2021; Xiong et al., 2020).

This work confirmed that AHLs existing in EPS from sludge were the key driver for enhanced CAP-degrading anode biofilm formation in our previous study (Wu et al., 2021). As most of reported studies applied commercially available AHLs which are very expensive, this study provides an economical strategy to regulate electrode biofilm formation by using the sludge EPS. In summary, the proposed mechanisms of AHLs in the sludge EPS for improved CAP-degrading anode biofilm acclimation were as follows: (1) AHLs facilitated the construction of a thick and 3D structured biofilm with high cell viability; (2) AHLs increased the PN/PS ratio and conductive contents in the EPS of the biofilm; (3) AHLs facilitated the formation of a biofilm with rich biodiversity and balanced bacterial proportions, leading to more beneficial mutualism among different functional bacteria; (4) AHLs specifically selected more bifunctional bacteria (for electricity generation and antibiotic resistance/degradation) in the biofilm.

4. Conclusions

In this study, we identified the key role of AHLs in the sludge EPS for enhanced CAP-degrading anode biofilm formation in MFCs. The AHL-manipulation during the anode biofilm acclimation could not only maintain stable voltage outputs but also significantly accelerate CAP removal in the MFC. The thick and 3D structured biofilm, strong and homogeneous cell viability throughout the biofilm, and high PN/PS ratio along with more conductive contents in the biofilm EPS conspired to cause the above improvements. In addition, AHLs facilitated the formation of a biofilm with rich biodiversity, balanced bacterial proportions, and more bifunctional bacteria. Since we determined AHLs in the sludge EPS, further research is required to investigate the regulation mechanisms of specific AHLs for CAP-degrading anode biofilm formation in MFCs.

Declaration of competing interest

The authors declare that they have no known competing financial interests or personal relationships that could have appeared to influence the work reported in this paper.

Acknowledgements

This work was financially supported by the National Key R & D Program of China (2018YFA0902200), the National Natural Science Foundation of China (21808108, 21808109), Postgraduate Research & Practice Innovation Program of Jiangsu Province (KYCX21_1085), the National Natural Science Foundation of Tianjin (18JCQNJC10200), Qing Lan Project of Jiangsu Universities, Six Talent Peaks Project in Jiangsu Province, the Jiangsu Synergetic Innovation Center for Advanced Bio-Manufacture, and the European Union's Horizon 2020 Research and Innovation Programme (GREENER, GA 826312).

Appendix A. Supplementary data

Supplementary data to this article can be found online at <https://doi.org/10.1016/j.envres.2021.112649>.

References

- Chatterjee, P., et al., 2019. Selective enrichment of biocatalysts for bioelectrochemical systems: a critical review. *Renew. Sustain. Energy Rev.* 109, 10–23.
- Chen, Q., et al., 2016. Long-term field application of sewage sludge increases the abundance of antibiotic resistance genes in soil. *Environ. Int.* 92–93, 1–10.
- Chen, S., et al., 2017. Quorum sensing signals enhance the electrochemical activity and energy recovery of mixed-culture electroactive biofilms. *Biosens. Bioelectron.* 97, 369–376.
- Cui, Y., et al., 2020. Biosynthesized iron sulfide nanoparticles by mixed consortia for enhanced extracellular electron transfer in a microbial fuel cell. *Bioresour. Technol.* 318, 124095.
- Dewan, K.K., et al., 2018. Development of macrolide resistance in *Bordetella bronchiseptica* is associated with the loss of virulence. *J. Antimicrob. Chemother.* 73, 2797–2805.
- Fang, Y., et al., 2018. Accelerating the start-up of the cathodic biofilm by adding acyl-homoserine lactone signaling molecules. *Bioresour. Technol.* 266, 548–554.
- Freguia, S., et al., 2009. *Lactococcus lactis* catalyses electricity generation at microbial fuel cell anodes via excretion of a soluble quinone. *Bioelectrochemistry* 76, 14–18.
- Guo, J., et al., 2016a. Rapid start-up of the anammox process: effects of five different sludge extracellular polymeric substances on the activity of anammox bacteria. *Bioresour. Technol.* 220, 641–646.
- Guo, N., et al., 2019. Mechanisms of metabolic performance enhancement during electrically assisted anaerobic treatment of chloramphenicol wastewater. *Water Res.* 156, 199–207.
- Guo, N., et al., 2017. Effect of bio-electrochemical system on the fate and proliferation of chloramphenicol resistance genes during the treatment of chloramphenicol wastewater. *Water Res.* 117, 95–101.
- Guo, W., et al., 2016b. Removal of chloramphenicol and simultaneous electricity generation by using microbial fuel cell technology. *Int. J. Electrochem. Sci.* 5128–5139.
- He, C.S., et al., 2020. Interactions between nanoscale zero valent iron and extracellular polymeric substances of anaerobic sludge. *Water Res.* 178, 115817.
- Herraiz-Carbone, M., et al., 2020. Improving the biodegradability of hospital urines polluted with chloramphenicol by the application of electrochemical oxidation. *Sci. Total Environ.* 725, 138430.
- Hu, H., et al., 2016. Role of N-acyl-homoserine lactone (AHL) based quorum sensing on biofilm formation on packing media in wastewater treatment process. *RSC Adv.* 6, 11128–11139.
- Hu, X., et al., 2020. N- and O self-doped biomass porous carbon cathode in an electro-Fenton system for chloramphenicol degradation. *Separ. Purif. Technol.* 251, 117376.
- Jia, F., et al., 2017. Stratification of extracellular polymeric substances (EPS) for aggregated anammox microorganisms. *Environ. Sci. Technol.* 51, 3260–3268.
- Klüpfel, L., et al., 2014. Humic substances as fully regenerable electron acceptors in recurrently anoxic environments. *Nat. Geosci.* 7, 195–200.
- Kong, D., et al., 2015. Cathodic degradation of antibiotics: characterization and pathway analysis. *Water Res.* 72, 281–292.
- Kong, F., et al., 2018. Enhanced azo dye decolorization and microbial community analysis in a stacked bioelectrochemical system. *Chem. Eng. J.* 354, 351–362.
- Kumar, A., et al., 2020. Carbon quantum dots and reduced graphene oxide modified self-assembled S@C₃N₄/B@C₃N₄ metal-free nano-photocatalyst for high performance degradation of chloramphenicol. *J. Mol. Liq.* 300, 112356.
- Kumar, S.S., et al., 2017. Effect of cathode environment on bioelectricity generation using a novel consortium in anode side of a microbial fuel cell. *Biochem. Eng. J.* 121, 17–24.
- Li, H., et al., 2019. Effects of graphite and Mn ore media on electro-active bacteria enrichment and fate of antibiotic and corresponding resistance gene in up flow microbial fuel cell constructed wetland. *Water Res.* 165, 114988.
- Li, S., et al., 2020. Degradation pathways, microbial community and electricity properties analysis of antibiotic sulfamethoxazole by bio-electro-Fenton system. *Bioresour. Technol.* 298, 122501.

- Li, T., et al., 2022. Quinones contained in wastewater as redox mediators for the synergistic removal of azo dye in microbial fuel cells. *J. Environ. Manag.* 301, 113924.
- Liang, B., et al., 2013. Accelerated reduction of chlorinated nitroaromatic antibiotic chloramphenicol by biocathode. *Environ. Sci. Technol.* 47, 5353–5361.
- Liu, X., et al., 2018a. Insight into the kinetics and mechanism of removal of aqueous chlorinated nitroaromatic antibiotic chloramphenicol by nanoscale zero-valent iron. *Chem. Eng. J.* 334, 508–518.
- Liu, Y., et al., 2018b. Effects of extracellular polymeric substances (EPS) and N-acyl-L-homoserine lactones (AHLs) on the activity of anammox biomass. *Int. Biodeterior. Biodegrad.* 129, 141–147.
- Lv, L., et al., 2021. Exogenous N-acyl-homoserine lactones promote the degradation of refractory organics in oligotrophic anaerobic granular sludge. *Sci. Total Environ.* 761, 143289.
- Ma, C., et al., 2020. Molecular mechanisms underlying lignocellulose degradation and antibiotic resistance genes removal revealed via metagenomics analysis during different agricultural wastes composting. *Bioresour. Technol.* 314, 123731.
- Ma, X., et al., 2019. Response of antibiotic resistance to the co-existence of chloramphenicol and copper during bio-electrochemical treatment of antibiotic-containing wastewater. *Environ. Int.* 126, 127–133.
- Maddela, N.R., et al., 2019. Roles of quorum sensing in biological wastewater treatment: a critical review. *Chemosphere* 221, 616–629.
- Ondon, B.S., et al., 2020. Simultaneous removal and high tolerance of norfloxacin with electricity generation in microbial fuel cell and its antibiotic resistance genes quantification. *Bioresour. Technol.* 304, 122984.
- Pan, J., et al., 2020. Enhanced quorum sensing of anode biofilm for better sensing linearity and recovery capability of microbial fuel cell toxicity sensor. *Environ. Res.* 181, 108906.
- Qin, S., et al., 2020. Different refractory organic substances degradation and microbial community shift in the single-chamber bio-photoelectrochemical system. *Bioresour. Technol.* 307, 123176.
- Ren, J., et al., 2021. Bioelectrochemical sulfate reduction enhanced nitrogen removal from industrial wastewater containing ammonia and sulfate. *AIChE J.* 67, e17309.
- Sun, D., et al., 2015. Temporal-spatial changes in viabilities and electrochemical properties of anode biofilms. *Environ. Sci. Technol.* 49, 5227–5235.
- Venkataraman, A., et al., 2010. Quorum sensing regulates electric current generation of *Pseudomonas aeruginosa* PA14 in bioelectrochemical systems. *Electrochem. Commun.* 12, 459–462.
- Wang, J., et al., 2021. AHLs-mediated quorum sensing threshold and its response towards initial adhesion of wastewater biofilms. *Water Res.* 194, 116925.
- Wu, X., et al., 2015. Effect of zeolite-coated anode on the performance of microbial fuel cells. *J. Chem. Technol. Biotechnol.* 90, 87–92.
- Wu, X., et al., 2021. Enhanced chloramphenicol-degrading biofilm formation in microbial fuel cells through a novel synchronous acclimation strategy. *J. Clean. Prod.* 317.
- Wu, X., et al., 2020. Effects of copper salts on performance, antibiotic resistance genes, and microbial community during thermophilic anaerobic digestion of swine manure. *Bioresour. Technol.* 300, 122728.
- Wu, X., et al., 2018. Anode modification by biogenic gold nanoparticles for the improved performance of microbial fuel cells and microbial community shift. *Bioresour. Technol.* 270, 11–19.
- Xiong, F., et al., 2020. Effects of N-acyl-homoserine lactones-based quorum sensing on biofilm formation, sludge characteristics, and bacterial community during the start-up of bioaugmented reactors. *Sci. Total Environ.* 735, 139449.
- Yan, W., et al., 2019. The effect of bioelectrochemical systems on antibiotics removal and antibiotic resistance genes: a review. *Chem. Eng. J.* 358, 1421–1437.
- Yang, G., et al., 2019. Anode potentials regulate *Geobacter* biofilms: new insights from the composition and spatial structure of extracellular polymeric substances. *Water Res.* 159, 294–301.
- Yun, H., et al., 2016. Response of anodic bacterial community to the polarity inversion for chloramphenicol reduction. *Bioresour. Technol.* 221, 666–670.
- Zhang, B., et al., 2018. The attachment potential and N-acyl-homoserine lactone-based quorum sensing in aerobic granular sludge and algal-bacterial granular sludge. *Appl. Microbiol. Biotechnol.* 102, 5343–5353.
- Zhang, J., et al., 2020a. High-efficiency biodegradation of chloramphenicol by enriched bacterial consortia: kinetics study and bacterial community characterization. *J. Hazard Mater.* 384, 121344.
- Zhang, Q., et al., 2020b. Exogenous extracellular polymeric substances as protective agents for the preservation of anammox granules. *Sci. Total Environ.* 747, 141464.
- Zhang, Q., et al., 2017. Cometabolic degradation of chloramphenicol via a meta-cleavage pathway in a microbial fuel cell and its microbial community. *Bioresour. Technol.* 229, 104–110.
- Zhang, S., et al., 2019a. Inhibition of methanogens decreased sulfadiazine removal and increased antibiotic resistance gene development in microbial fuel cells. *Bioresour. Technol.* 281, 188–194.
- Zhang, W., et al., 2020c. Power to hydrogen-oxidizing bacteria: effect of current density on bacterial activity and community spectra. *J. Clean. Prod.* 263, 121596.
- Zhang, X., et al., 2020d. Electrodes bioaugmentation promotes the removal of antibiotics from concentrated sludge in microbial electrolysis cells. *Sci. Total Environ.* 715, 136997.
- Zhang, Z., et al., 2019b. The regulation of N-acyl-homoserine lactones (AHLs)-based quorum sensing on EPS secretion via ATP synthetic for the stability of aerobic granular sludge. *Sci. Total Environ.* 673, 83–91.
- Zhao, X., et al., 2019. Shifting interactions among bacteria, fungi and archaea enhance removal of antibiotics and antibiotic resistance genes in the soil bioelectrochemical remediation. *Biotechnol. Biofuels* 12, 160.
- Zhu, M., et al., 2020. Microbial network succession along a current gradient in a bio-electrochemical system. *Bioresour. Technol.* 314, 123741.
- Zhu, Y.G., et al., 2017. Continental-scale pollution of estuaries with antibiotic resistance genes. *Nat. Microbiol.* 2, 16270.